

Article

Efficient Oxidation of Methyl Glycolate to Methyl Glyoxylate Using a Fusion Enzyme of Glycolate Oxidase, Catalase and Hemoglobin

Xiangxian Ying ^{1,*} , Can Wang ¹, Shuai Shao ¹, Qizhou Wang ¹, Xueting Zhou ¹, Yanbing Bai ², Liang Chen ², Chenze Lu ³, Man Zhao ¹  and Zhao Wang ¹

¹ Key Laboratory of Bioorganic Synthesis of Zhejiang Province, College of Biotechnology and Bioengineering, Zhejiang University of Technology, Hangzhou 310014, China; m17816035735@163.com (C.W.); ss1964241742@163.com (S.S.); W2936716405@163.com (Q.W.); sadie598851321@163.com (X.Z.); mzhao@zjut.edu.cn (M.Z.); hzwangzhao@zjut.edu.cn (Z.W.)

² Hangzhou Xinfu Science & Technology Co., Ltd., Hangzhou 311301, China; byb@xinfupharm.com (Y.B.); chenliang201006@163.com (L.C.)

³ College of Life Sciences, China Jiliang University, Hangzhou 310018, China; chenzelu@cjlu.edu.cn

* Correspondence: yingxx@zjut.edu.cn; Tel.: +86-571-88320781

Received: 3 August 2020; Accepted: 13 August 2020; Published: 17 August 2020



Abstract: Possessing aldehyde and carboxyl groups, glyoxylic acid and its ester derivatives serve as platform chemicals for the synthesis of vanillin, (*R*)-pantolactone, antibiotics or agrochemicals. Methyl glycolate is one of the by-products in the coal-to-glycol industry, and we attempted its value-added use through enzymatic oxidation of methyl glycolate to methyl glyoxylate. The cascade catalysis of glycolate oxidase from *Spinacia oleracea* (*SoGOX*), catalase from *Helicobacter pylori* (*HpCAT*) and hemoglobin from *Vitreoscilla stercoraria* (*VsHGB*) was firstly constructed, despite poor catalytic performance. To enable efficient oxidation of methyl glycolate, eight fusion enzymes of *SoGOX*, *HpCAT* and *VsHGB* were constructed by varying the orientation and the linker length. The fusion enzyme *VsHGB-GSG-SoGOX-GGGGS-HpCAT* was proved to be best, which reaction yield was 2.9 times higher than that of separated enzymes. The enzyme *SoGOX* was further subjected to directed evolution and site-saturation mutagenesis. The reaction yield of the resulting variant M267T/S362G was 1.9 times higher than that of the wild type. Then, the double substitution M267T/S362G was integrated with fusion expression to give the fusion enzyme *VsHGB-GSG-SoGOX^{mut}-GGGGS-HpCAT*, which crude enzyme was used as biocatalyst. The use of crude enzyme virtually eliminated side reactions and simplified the preparation of biocatalysts. Under the optimized conditions, the crude enzyme *VsHGB-GSG-SoGOX^{mut}-GGGGS-HpCAT* catalyzed the oxidation of 200 mM methyl glycolate for 6 h, giving a yield of 95.3%. The development of efficient fusion enzyme and the use of its crude enzyme paved the way for preparative scale application on enzymatic oxidation of methyl glycolate to methyl glyoxylate.

Keywords: methyl glyoxylate; glycolate oxidase; catalase; hemoglobin; fusion expression; directed evolution; cascade catalysis

1. Introduction

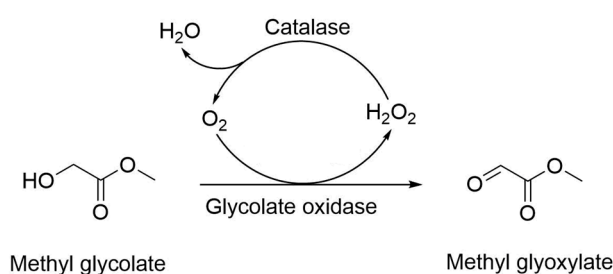
Esters of glyoxylic acid with both aldehyde and carboxyl groups serve as platform chemicals for producing a large portfolio of products in perfume, pharmaceutical and agrochemical industries [1–4]. For example, glyoxylate esters serve as one of the starting materials in the synthesis of (*R*)-pantolactone, the key industrial intermediate for the production of D-pantothenate [5]. Methyl glycolate is a by-product originating from incomplete reduction of dimethyl oxalate in the coal-to-glycol industry.

With the maturity of coal-to-glycol technology, high-value use of methyl glycolate has been becoming urgent. As one of alcohols, methyl glycolate can be oxidized to methyl glyoxylate through chemical or enzymatic approach, and methyl glyoxylate can be further hydrolyzed to glyoxylic acid if necessary. Chemical oxidation of alcohols to the corresponding aldehydes usually requires metal catalysts and often causes over-oxidation. In contrast to the chemical methods, enzymatic oxidation of alcohols is milder and greener, and can reduce the side reactions [6–8].

In the enzymatic oxidation of glycolate to glyoxylate, biocatalysts in common use include alcohol oxidases and alcohol dehydrogenases [9–12]. Glycolate dehydrogenases catalyze the dehydrogenation of glycolate to glyoxylate in the presence of nicotinamide coenzyme, requiring the addition of expensive nicotinamide coenzyme and efficient coenzyme regeneration. Meanwhile, glycolate oxidases together with oxygen catalyze the oxidation of glycolate to produce glyoxylate and hydrogen peroxide [13]. Although both alcohol dehydrogenases and alcohol oxidases could be competent, glycolate oxidase-catalyzed oxidation appears more suitable since oxygen is the cheapest oxidant and the process yields fewer waste products [14].

For efficient alcohol oxidase-catalyzed oxidation, the cascade catalysis of alcohol oxidase and catalase is usually essential to decompose the harmful by-product H_2O_2 into water and oxygen [15–17]. The tandem use of alcohol oxidase together with hemoglobin is also an effective approach for improving the catalytic activity of oxygen-consuming enzymes, relying on the oxygen binding and releasing capability of hemoglobin [6,18]. In enzymatic cascade catalysis, linking genes for the fusion expression of multiple enzymes was worthy of consideration, and enabled better catalytic performance than the separate enzymes [19]. Recently, the number of successful examples for the fusion expression of alcohol oxidase and other enzymes is considerably increasing [19]. In addition, protein engineering has been proved to be powerful for overcoming the deficiencies of native redox enzymes [20]. To engineer the enzymes, rational design requires detailed knowledge about structure function relationships, whereas directed evolution can improve an enzyme's properties with virtually no structural knowledge [21]. Although the knowledge of the structure function relationships of glycolate oxidase is accumulating, the uncertainty on the catalysis nature of glycolate oxidase remains significant [13]. Thus, directed evolution seems to be more feasible for improving the properties of glycolate oxidase.

In contrast to the oxidation of glycolic acid, the oxidation of methyl glycolate has the advantages of less pH change, easy product isolation, and direct process integration for subsequent organic synthesis. To the best of our knowledge, this is the first attempt to fulfill enzymatic oxidation of methyl glycolate to methyl glyoxylate. To achieve efficient oxidation of methyl glycolate, glycolate oxidase from *Spinacia oleracea* (SoGOX) [9], catalase from *Helicobacter pylori* (HpCAT) [22] and hemoglobin from *Vitreoscilla stercoraria* (VsHGB) [23] were firstly chosen to construct the cascade catalysis (Scheme 1). Furthermore, the fusion expression bringing SoGOX, HpCAT and VsHGB together was fulfilled to enhance the catalytic performance of cascade catalysis. In addition, we conducted the direct evolution of the key enzyme SoGOX toward its activity improvement. Finally, the integration of multiple improvements enabled efficient enzymatic oxidation of methyl glyoxylate (>200 mM) with 6 h oxidation.



Scheme 1. Oxidation of methyl glycolate to methyl glyoxylate through cascade catalysis of glycolate oxidase, catalase and hemoglobin. In the cascade catalysis, the hemoglobin facilitated the reaction through the binding and releasing of oxygen.

2. Results and Discussion

2.1. Cascade Catalysis of Glycolate Oxidase, Catalase and Hemoglobin

Spinach glycolate oxidase SoGOX has been well characterized on the oxidation of glycolate to glyoxylate [24–27]. Rather than glycolic acid, methyl glycolate was tested as a substrate in this study. The gene encoding SoGOX was successfully over-expressed in *E. coli*, and the crude enzyme SoGOX was prepared (Figure 1). The crude enzyme SoGOX catalyzed the 24 h oxidation of methyl glycolate, only giving the yield of 21.1% (Table 1). The substrate and product in the alcohol oxidation were validated by GC-MS analyses (Figure S1). To fulfill efficient oxidation of methyl glyoxylate, the recombinant strains co-expressing glycolate oxidase SoGOX, catalase HpCAT and/or hemoglobin VsHGB were further constructed and induced (Figure 1). The crude extract from the cells co-expressing SoGOX and HpCAT catalyzed the same oxidation and resulted in the yield of 58.3%, indicating that the dismutation of H₂O₂ helped to promote alcohol oxidation. The use of the crude extract from the strain co-expressing SoGOX, HpCAT and VsHGB increased the yield up to 65.2%, suggesting the introduction of hemoglobin was good for alcohol oxidation. Due to the limited solubility of oxygen in water, oxygen supply was pivotal for the oxidation catalyzed by oxygen-dependent enzymes [6]. Thus, the yield was as high as 88.7% when the reaction mixture was aerated with pure oxygen at a flow rate of 1 L/h (Table 1).

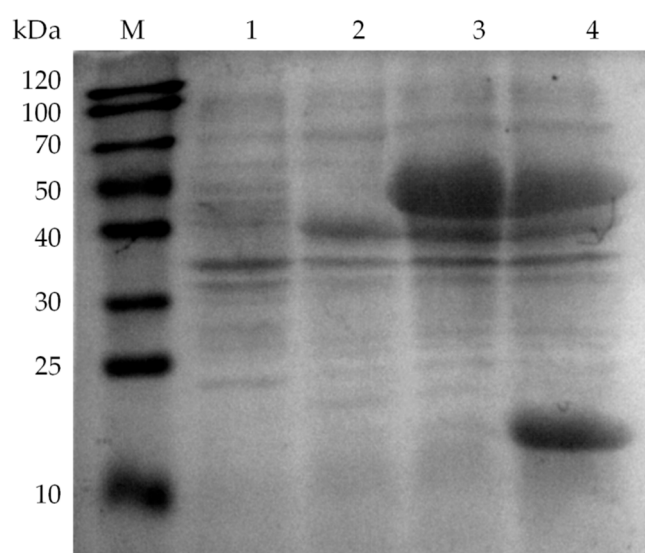


Figure 1. SDS-PAGE analysis of glycolate oxidase SoGOX, catalase HpCAT and/or hemoglobin VsHGB in the crude extracts. Lane M, marker; lane 1, no induction of the cells co-expressing SoGOX, HpCAT or VsHGB as the control; lane 2, expression of SoGOX (~40 kDa) alone; lane 3, co-expression of SoGOX and HpCAT (~54 kDa); lane 4, co-expression of SoGOX, HpCAT and VsHGB (~16 kDa). The crude extract samples were run by PAGE (12% acrylamide) and stained with Coomassie Brilliant Blue R-250.

Table 1. Oxidation of methyl glycolate to methyl glyoxylate catalyzed by crude extracts expressing SoGOX, HpCAT and/or VsHGB¹.

The Protein(s) Expressed in <i>E. coli</i> Cells	Yield (%)
SoGOX	21.1 ± 0.5
SoGOX and HpCAT	58.3 ± 1.3
SoGOX, HpCAT and VsHGB	65.2 ± 2.1
SoGOX, HpCAT and VsHGB ²	88.7 ± 2.5

¹ The reaction mixture (5 mL) contained 10 mg crude enzyme, 100 mM methyl glycolate, 0.01 mM FMN and 50 mM Tris-HCl (pH 8.0). The reaction was carried out at 25 °C and 600 rpm for 24 h. ² The aeration rate of oxygen was 1 L/h.

2.2. Fusion Expression of Glycolate Oxidase, Catalase and Hemoglobin

In redox reactions, the fusion of multiple enzymes could be powerful for generating proteins with improved activity and stability [19]. Assuming that the fusion of SoGOX, HpCAT and VsHGB could make for improving the oxidation of methyl glycolate, linking the genes encoding VsHGB, SoGOX and HpCAT with the linker GSG was initially conducted and the resulting fusion gene was successfully induced (Figure 2). The catalysis of crude enzyme VsHGB-GSG-SoGOX-GSG-HpCAT showed that its yield of 57.6% was significantly higher than those of SoGOX alone (12.8%) and non-fusion co-expression of SoGOX, HpCAT and VsHGB (23.6%) (Figure 3). The organization of the fusions, including the orientation and the length of the linker, was critical for the catalytic performance [28,29]. Following similar procedure for the construction of VsHGB-GSG-SoGOX-GSG-HpCAT, the other seven fusion enzymes were constructed, induced and then visualized through SDS-PAGE analyses (Figure 2). The enzyme SoGOX expressed in *E. coli* was predominately in the form of inclusion bodies (data not shown), whereas the over-expression of VsHGB and HpCAT in *E. coli* was fully soluble (Figure 1). In contrast to the non-fusion co-expression of VsHGB, SoGOX and HpCAT, all eight fusion enzymes of VsHGB, SoGOX and HpCAT exhibited higher soluble expression level (Figure 2), suggesting that the organization of SoGOX flanking with the partners VsHGB and HpCAT might improve the structural folding [28]. All the resulting fusion enzymes exhibited much better catalytic performance for alcohol oxidation than separated enzymes (23.6% yield) (Figure 3). The organization VsHGB-GSG-SoGOX-GGGGS-HpCAT was demonstrated to be the best, converting 100 mM methyl glycolate to methyl glyoxylate with a yield of 67.8% after 4 h oxidation.

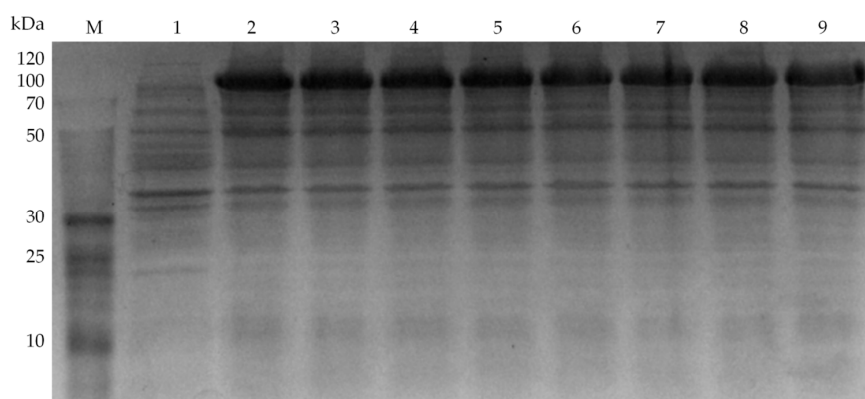


Figure 2. SDS-PAGE analysis of eight fusion proteins with different organizations. Lane M, protein marker; lane 1, no induction of the fusion enzyme as the control; lane 2, VsHGB-GSG-SoGOX-GSG-HpCAT; lane 3, VsHGB-GSG-SoGOX-GGGGS-HpCAT; lane 4, VsHGB-GGGGS-SoGOX-GSG-HpCAT; lane 5, VsHGB-GGGGS-SoGOX-GGGGS-HpCAT; lane 6, HpCAT-GSG-SoGOX-GSG-VsHGB; lane 7, HpCAT-GSG-SoGOX-GGGGS-VsHGB; lane 8, HpCAT-GGGGS-SoGOX-GSG-VsHGB; lane 9, HpCAT-GGGGS-SoGOX-GGGGS-VsHGB. The crude enzyme samples were run by PAGE (12% acrylamide) and stained with Coomassie Brilliant Blue R-250.

2.3. Directed Evolution of Glycolate Oxidase

During the cascade catalysis of SoGOX and HpCAT, the activity of SoGOX was considerably lower than that of HpCAT [15]. It is reasonable to expect that the activity improvement of SoGOX would increase the efficiency of cascade catalysis. The directed evolution of SoGOX was performed to generate the first round of mutant library by error-prone PCR. The primary screening of mutants was judged on the evolved H₂O₂ accompanied by alcohol oxidation. In the detection of H₂O₂, H₂O₂ oxidized Fe²⁺ to Fe³⁺, which then combined with dye molecules to produce purple Fe³⁺-dye complexes [30]. The concentrations of H₂O₂ were measured by determining the absorbance at 595 nm. Seven mutants (7-A6, 13-H5, 15-F10, 15-G2, 20-C7, 22-H3 and 31-D12) showing higher concentration of H₂O₂ than the wild type, were obtained from over 8000 clones of mutant library (Table 2). The positive

mutants were further verified through HPLC analysis of the reaction mixture of alcohol oxidation. Except for the mutant 22-H3, all the other mutants increased catalytic activities to some extent (108.3–153.3%) (Figure 4). Among them, the yield of the mutant 20-C7 with double substitutions of M267S/S362G showed 1.53 times higher than that of the wild type. Then, the sites M267 and S362 were further subjected to generate the second round of mutant library by site-saturation mutagenesis. After the screening of about 800 clones, the selected variants M267S/S362A and M267T/S362G exhibited better catalytic performance than that of the wild type, judging on both the evolved H₂O₂ and the yield of methyl glyoxylate. Particularly, the catalytic performance of the variant M267T/S362G designated as SoGOX^{mut} was even superior to that of the variant M267S/S362G (Table 3). Similar to the latest engineering of *Aerococcus viridans* L-lactate oxidase [31], both sites M267 and S362 were located on the surface of SoGOX (Figure S2), and the site S362 was very close to the C-terminal of SoGOX. Engineering the polar residues on the surface of *Aerococcus viridans* L-lactate oxidase changed electrostatic interaction, oxygen accessible tunnel and the distance of FMN N5 and C α of the modified residue. Unfortunately, our docking analyses could not establish the sound relationship between the activity improvement and the residue substitution, warranting more efforts for the interpretation of structure-function relationships.

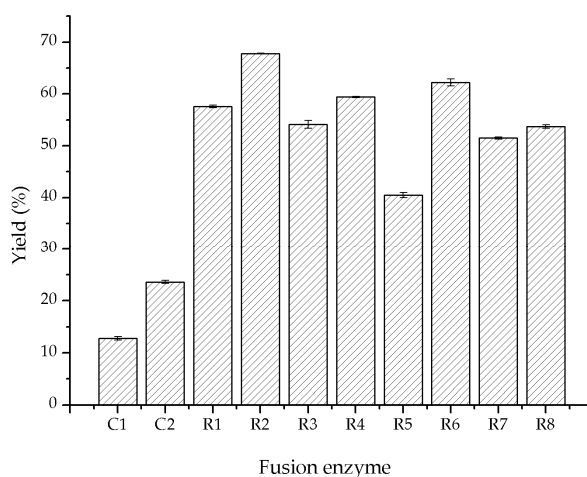


Figure 3. Comparison of different fusion enzymes on catalytic performance of alcohol oxidation. C1, SoGOX alone as the control; C2, the control co-expressing SoGOX, HpCAT and VsHGB separately; R1, VsHGB-GSG-SoGOX-GSG-HpCAT; R2, VsHGB-GSG-SoGOX-GGGGS-HpCAT; R3, VsHGB-GGGGS-SoGOX-GSG-HpCAT; R4, VsHGB-GGGGS-SoGOX-GGGGS-HpCAT; R5, HpCAT-GSG-SoGOX-GSG-VsHGB; R6, HpCAT-GSG-SoGOX-GGGGS-VsHGB; R7, HpCAT-GGGGS-SoGOX-GSG-VsHGB; R8, HpCAT-GGGGS-SoGOX-GGGGS-VsHGB. The reaction mixture (5 mL) contained 10 mg crude enzyme, 100 mM methyl glycolate, 0.01 mM FMN and 50 mM Tris-HCl (pH 8.0). The reaction at an oxygen aeration rate of 1 L/h was carried out at 25 °C and 600 rpm for 4 h.

Table 2. Comparison of the wild type and the mutants on the concentration of evolved H₂O₂¹.

Mutant	Amino Acid Substitution	H ₂ O ₂ (μM)
WT		45.5
7-A6	I73V	61.2
13-H5	R134H/K169R	71.2
15-F10	A138L/Y261F	67.9
15-G2	K190S	66.9
20-C7	M267S/S362G	80.6
22-H3	S314T	59.1
31-D12	K274S	69.4

¹ The reaction mixture (500 μL) in a 96-well plate contained around 100 μL cell lysate, 100 mM methyl glycolate and 50 mM Tris-HCl (pH 8.0). The reaction was carried out at 37 °C and 200 rpm for 8 h.

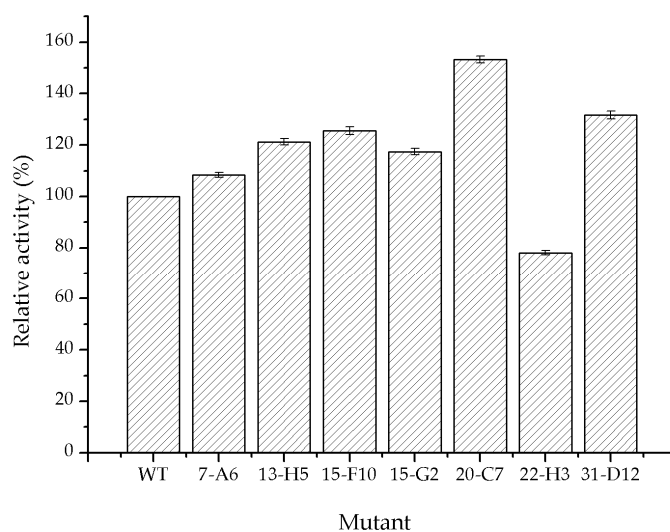


Figure 4. Comparison of the wild type and the mutants on catalytic performance of alcohol oxidation. The reaction mixture (5 mL) contained 10 mg crude enzyme, 100 mM methyl glycolate, 0.01 mM FMN and 50 mM Tris-HCl (pH 8.0). The reaction at an oxygen aeration rate of 1 L/h was carried out at 25 °C and 600 rpm for 8 h.

Table 3. Comparison of the wild type and its double-substitution variants on the concentration of evolved H₂O₂ and catalytic performance of alcohol oxidation.

Combinatorial Mutant	H ₂ O ₂ (μM) ¹	Yield (%) ²
WT	45.5	26.3
M267S/S362G	80.6	45.3
M267S/S362A	54.5	33.7
M267T/S362G	96.7	50.1

¹ The reaction mixture (500 μL) in a 96-well plate contained around 100 μL cell lysate, 100 mM methyl glycolate and 50 mM Tris-HCl (pH 8.0). The reaction was carried out at 37 °C and 200 rpm for 8 h. ² The reaction mixture (5 mL) contained 10 mg crude enzyme, 100 mM methyl glycolate, 0.01 mM FMN and 50 mM Tris-HCl (pH 8.0). The reaction at an oxygen aeration rate of 1 L/h was carried out at 25 °C and 600 rpm for 24 h.

2.4. Investigation of Key Factors on Oxidation of Methyl Glycolate to Methyl Glyoxylate

To integrate the improvements of the fusion expression and directed evolution, the double substitutions M267S and S362G were introduced into the fusion enzyme *VsHGB-GSG-SoGOX-GGGGS-HpCAT*, yielding the fusion enzyme *VsHGB-GSG-SoGOX^{mut}-GGGGS-HpCAT*. When tested under the same catalytic conditions, the reaction yield of crude enzyme *VsHGB-GSG-SoGOX^{mut}-GGGGS-HpCAT* was 1.2 times higher than that of crude enzyme *VsHGB-GSG-SoGOX-GGGGS-HpCAT*. Hence, crude enzyme *VsHGB-GSG-SoGOX^{mut}-GGGGS-HpCAT* was used as biocatalyst for subsequent the orchestration of reaction conditions. During cascade biocatalysis, the enzymes *SoGOX^{mut}*, *HpCAT* and *VsHGB* run in the same pot and the optimal conditions of each enzyme are usually not be met [16]. Thus, we investigated various factors affecting alcohol oxidation, including temperature, pH, aeration rate of oxygen, the concentration of FMN and the substrate concentration. The fusion enzyme was active over a range of 5–40 °C, and the highest yield (70.35%) was observed at 15 °C (Figure 5a). Higher temperature (>15 °C) decreased the product yield. Since *HpCAT* was a moderately thermostable enzyme [22], the thermal optimum was mainly associated with that of *SoGOX^{mut}*. The optimal pH of alcohol oxidation was tested at the pH values ranging from 6.0 to 10.0 at 15 °C. The optimal pH was observed to be pH 8.0 (Figure 5b), at which spontaneous hydrolysis of methyl glycolate was kept at a relatively low level (<2%) (date not shown). The effect of oxygen supply was determined by varying the aeration rate of oxygen from 0 to 3 L/h, and the optimal aeration rate was proved to be 1 L/h (Figure 5c). *SoGOX* is FMN-dependent and the effect of FMN was investigated by supplementing

exogenous FMN from 0 to 0.2 mM. Under the tested conditions, the addition of exogenous FMN had no benefit for the oxidation of methyl glycolate, suggesting endogenous FMN met for the requirement of the oxidation of methyl glycolate (Figure 5d). When the substrate concentration increased from 50 to 200 mM, the yields were kept at a high level (>95%) (Figure 5e). A further increase of substrate concentration to 400 mM resulted in a sharp decrease in the yields, which might be attributed to the enzyme inactivation originated from higher concentrations of hydrophobic compounds and the accumulation of aldehyde toxicity [32]. Last but not least, the efforts of protein engineering toward further improvement of *SoGOX* activity and aldehyde tolerance are ongoing in our laboratory.

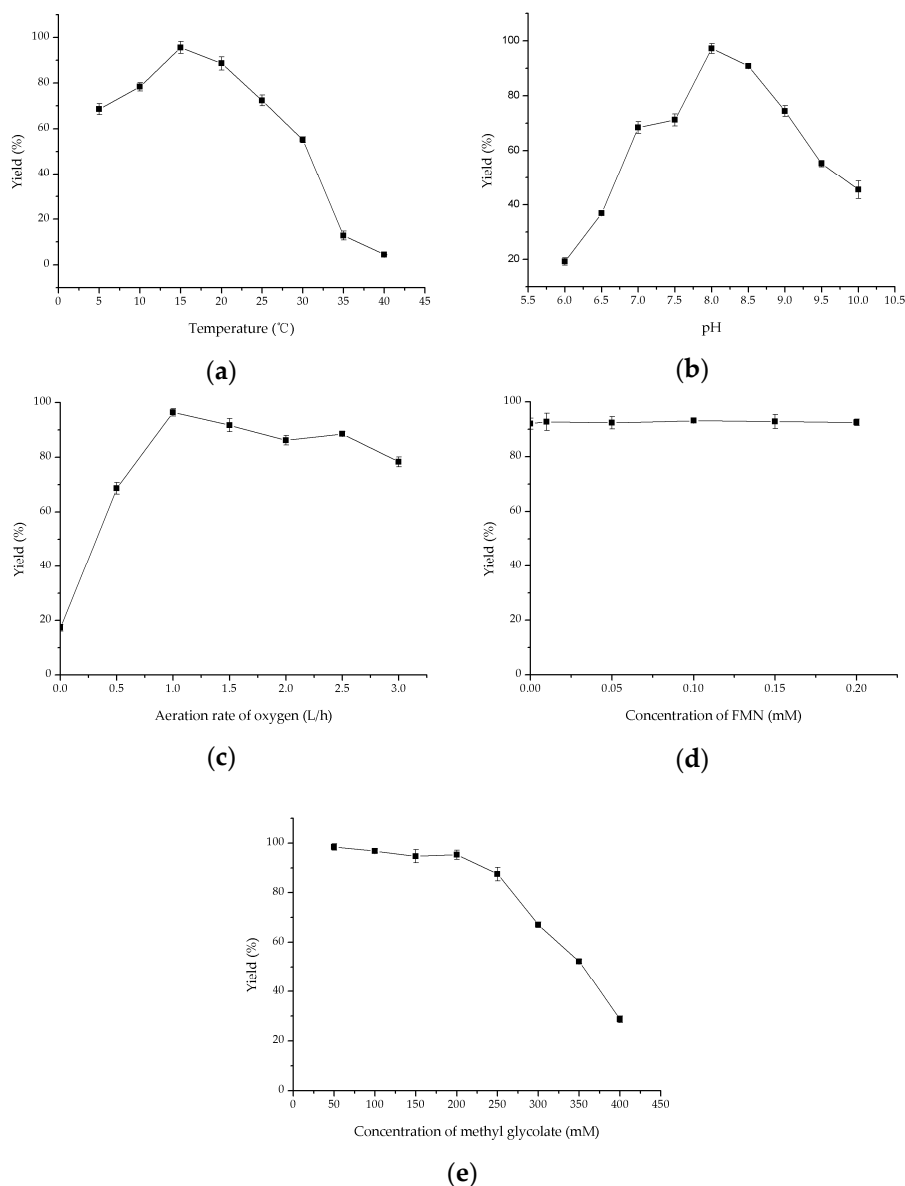


Figure 5. Factors affecting the oxidation of methyl glycolate to methyl glyoxylate: (a) Temperature; (b) pH; (c) the aeration rate of oxygen; (d) the concentration of FMN; (e) the substrate concentration. The reaction mixture (5 mL) contained 10 mg crude enzyme *VsHGB-GSG-SoGOX^{mut}-GGGGS-HpCAT*, 100 mM methyl glycolate, 0.01 mM FMN and 50 mM Tris-HCl (pH 8.0). The reaction at an oxygen aeration rate of 1 L/h was carried out at 15 °C and 600 rpm for 6 h. Then, the factors were individually varied to investigate the effect on the oxidation of methyl glycolate.

3. Materials and Methods

3.1. Genes, Organisms and Chemicals

The codon-optimized genes encoding *SoGOX* (GenBank accession number: ABY61829.1), *HpCAT* (GenBank accession number: AHY00946.1) and *VsHGB* (GenBank accession number: AKT95196.1) were synthesized by Tsingke Biotechnology Co., Ltd. (Hangzhou, China). The expression vectors used for over-expression included the plasmids pET28a and pACYC Duet-1. The strains *E. coli* DH5 α and *E. coli* BL21 (DE3) were used as the host for cloning and over-expression, respectively.

Methyl glyoxylate was supplied by Hangzhou Xinfu Science & Technology Co., Ltd. (Hangzhou, China). The suppliers for other chemicals of analytical grade included Sangon Biotech Co. Ltd. (Shanghai, China) and Sigma-Aldrich (Shanghai, China). The kits used for the determination of H₂O₂ and the manipulation of error-prone PCR were purchased from Sangon Biotech Co. Ltd. (Shanghai, China) and Tiandz, Inc. (Beijing, China), respectively. The ClonExpress MultiS One Step Cloning Kit was purchased from Vazyme Biotech Co., Ltd. (Nanjing, China).

3.2. Over-Expression of Glycolate Oxidase, Catalase and Hemoglobin

The gene encoding *SoGOX* was inserted into the sites *EcoR* I/*Hind* III of the vector pET28a, and the resulting plasmid was designated as pET28a-*SoGOX*. The recombinant plasmid pET28a-*SoGOX* was transformed into the host strain *E. coli* BL21(DE3), giving the recombinant strain *E. coli* BL21(DE3)/pET28a-*SoGOX*. Following the similar procedures, the recombinant strains *E. coli* BL21(DE3)/pET28a-*HpCAT* and *E. coli* BL21(DE3)/pET28a-*VsHGB* were constructed for the over-expression of *HpCAT* and *VsHGB*, respectively. Moreover, the gene encoding *HpCAT* was inserted into the sites *Nco* I/*Hind* III of the vector pACYC Duet-1, and the resulting plasmid was designated as pACYC Duet-1-*HpCAT*. The co-expression of *SoGOX* and *HpCAT* was fulfilled by transforming both pET28a-*SoGOX* and pACYC Duet-1-*HpCAT* into the same host strain *E. coli* BL21(DE3), and the resulting strain was designated as *E. coli* BL21(DE3)/pET28a-*SoGOX*/pACYC Duet-1-*HpCAT*. Similarly, the gene encoding *VsHGB* was inserted into the sites *Nde* I/*Xho* I of the plasmid pACYC Duet-1-*HpCAT*, and the resulting plasmid was designated as pACYC Duet-1-*HpCAT*-*VsHGB*. The co-expression of *SoGOX*, *HpCAT* and *VsHGB* was fulfilled by transforming both pET28a-*SoGOX* and pACYC Duet-1-*HpCAT*-*VsHGB* into the same host strain *E. coli* BL21(DE3), and the resulting strain was named as *E. coli* BL21(DE3)/pET28a-*SoGOX*/pACYC Duet-1-*HpCAT*-*VsHGB*.

The LB medium containing 50 μ g/mL antibiotics was routinely used for culturing the recombinant *E. coli* strains at 37 °C until the OD₆₀₀ of 0.6–0.8. Specifically, the strains containing the vector pACYC Duet-1 required 50 μ g/mL chloramphenicol, the strains containing the vector pET28a needed 50 μ g/mL kanamycin, meanwhile the cells containing both pACYC Duet-1 and pET28a demanded both 50 μ g/mL chloramphenicol and 50 μ g/mL kanamycin. The induction of the strains was initiated by the addition of 0.2 mM IPTG and then they were cultured at 25 °C for 12 h. At the end of incubation, the cells were washed twice using Tris-HCl buffer (50 mM, pH 8.0), harvested by 8000 \times *g* centrifugation at 4 °C for 10 min and stored at –20 °C for further use. A 12% (*w/v*) SDS-polyacrylamide gel electrophoresis (SDS-PAGE) was used to visualize the over-expression of *SoGOX*, *HpCAT* and *VsHGB*.

3.3. Fusion Expression of Glycolate Oxidase, Catalase and Hemoglobin

The fusion genes encoding *SoGOX*, *HpCAT* and *VsHGB* were assembled by multiple overlap extension PCR [33]. Multiple overlap extension PCR included two rounds of PCRs: the first round was to introduce the linkers (GSG or GGGGS) and overlap regions flanking each individual gene, and the second round was to assembly three genes from the first round of PCR into linear fragment. The construction of the fusion gene encoding *VsHGB*-GSG-*SoGOX*-GSG-*HpCAT* was used as an example to elucidate the procedure (Figure S3). Using the pair of primers pET28a-*VsHGB*-F and *VsHGB*-GSG-R (Table S1), the overlap region to pET28a was introduced to the upstream of *VsHGB* and the linker GSG together with the overlap region to *SoGOX* was introduced to the downstream of

VsHGB. Similarly, the gene encoding SoGOX was situated between the linker GSG together with the overlap region to VsHGB and the linker GSG together with the overlap region to HpCAT using the pair of primers GSG-SoGOX-F and SoGOX-GSG-R; the gene encoding HpCAT was flanked by the linker GSG together with the overlap region to SoGOX and the overlap region to pET28a using the pair of primers GSG-HpCAT-F and pET28a-HpCAT-R (Table S1). The plasmid pET28a-SoGOX, pET28a-HpCAT or pET28a-VsHGB served as the corresponding template. The PCR program was composed of the following steps: a 5 min period at 95 °C, 30 cycles of 95 °C (10 s), 58 °C (10 s) and 72 °C (30 s), and a final 5 min extension at 72 °C. The PCR products were purified and then used as the template in the second round of PCR. In the second round of PCR, the primers used were pET28a-VsHGB-F and pET28a-HpCAT-R (Table S1). The PCR program was composed of the following steps: a 5 min period at 95 °C, 30 cycles of 95 °C (15 s), 58 °C (30 s) and 72 °C (60 s), and a final 10 min extension at 72 °C. The fusion gene encoding VsHGB-GSG-SoGOX-GSG-HpCAT was confirmed by sequencing. In addition, the linear pET28a fragment was amplified by reverse PCR using the pair of primers pET28a-F and pET28a-R. The PCR products were digested by *Dpn* I to remove the template and then purified. Through Exnase II-driven homologous recombination in the ClonExpress MultiS One Step Cloning Kit, the gene encoding VsHGB-GSG-SoGOX-GSG-HpCAT and the linear pET28a fragment were ligated to form the recombinant plasmid pET28a-VsHGB-GSG-SoGOX-GSG-HpCAT. Following the same procedures, the total eight recombinant plasmids were created for the construction of fusion enzymes with different organizations, including pET28a-VsHGB-GSG-SoGOX-GSG-HpCAT, pET28a-VsHGB-GSG-SoGOX-GGGGS-HpCAT, pET28a-VsHGB-GGGGS-SoGOX-GSG-HpCAT, pET28a-VsHGB-GGGGS-SoGOX-GGGGS-HpCAT, pET28a-HpCAT-GSG-SoGOX-GSG-VsHGB, pET28a-HpCAT-GSG-SoGOX-GGGGS-VsHGB, pET28a-HpCAT-GGGGS-SoGOX-GSG-VsHGB and pET28a-HpCAT-GGGGS-SoGOX-GGGGS-VsHGB. All the primers used are listed in Tables S1 and S2. Each recombinant plasmid was transformed into the host strain *E. coli* BL21(DE3), and the resulting strain was grown in LB medium containing 50 µg/mL kanamycin. After the induction of the fusion enzyme, each crude fusion enzyme was prepared and then visualized through SDS-PAGE analyses.

3.4. Directed Evolution of Glycolate Oxidase SoGOX and Screening of the Evolved Mutants

Error-prone PCR was performed to generate randomly mutated SoGOX gene. The 50 µL of PCR reaction mixture contained 5 µL 10 × buffer, 0.4 µM each of primers (SoGOX-F and SoGOX-R, Table S3), 25 ng template (plasmid pET28a-SoGOX), 1 mM dNTPs, 1 mM dTTP and dCTP, 2.5 units of Taq DNA polymerase, and 0.5 mM MnCl₂. The PCR program was composed of the following steps: a 3 min period at 94 °C, 30 cycles of 94 °C (60 s), 56 °C (60 s) and 72 °C (60 s). The PCR products were digested by *Dpn* I to remove the template and then purified. The linear vector fragment was obtained by reverse PCR using the pair of primer pET28a-F and pET28a-R (Table S3). The PCR products were digested by *Dpn* I to remove the template and then purified. After that, the PCR products and the linear vector fragment were ligated into the recombinant plasmids using the ClonExpress MultiS One Step Cloning Kit. The recombinant plasmids were transformed into the host *E. coli* BL21(DE3) for primary screening of activity-improved mutants.

A colorimetric assay was used for primary screening of the evolved mutants [30]. The oxidation of methyl glycolate produced methyl glyoxylate and H₂O₂. Thus, the detection of H₂O₂ could reflect the level of glycolate oxidase activity. Using the kit of H₂O₂ determination, H₂O₂ oxidized Fe²⁺ to Fe³⁺, which then combined with dye molecules to produce purple Fe³⁺-dye complexes. The concentrations of H₂O₂ were measured by detecting the absorbance at 595 nm (Figure S4). Transformants from the mutant library were incubated in a 96-deep well plate (Qiagen, Hilden, Germany) with each well containing 500 µL of liquid LB medium and 100 µg/mL kanamycin. After an overnight growth at 37 °C, 10 µL culture was inoculated into another 500 µL fresh LB culture containing 0.2 mM IPTG and 100 µg/mL kanamycin, followed by 12 h induction at 25 °C and 150 rpm. After that, the culture was centrifuged at 8000× g for 10 min and the supernatant was discarded. Then, the cells were re-suspended using 100 µL cell-lysis solution (Tris-HCl buffer, pH 8.0, 1 mg/mL lysozyme, 2 mM EDTA,

100 mM NaCl and 0.5% Triton X-100) and three cycles of freeze-thawing were conducted to disrupt the cells. After the centrifugation of $4000\times g$ for 20 min, the supernatant was used as the crude enzyme. The crude enzyme in the 96-deep well plate was transferred and mixed with methyl glycolate at a final concentration of 100 mM. After the reaction at 37 °C for 8 h, 20 μ L reaction mixture was mixed with 200 μ L colorimetric solution. The absorbance at 595 nm was determined with a spectrophotometer (Thermo Scientific, Shanghai, China) after 30 min colorimetric reaction at 25 °C, mutants exhibiting a higher absorbance than the control were picked out for further verification (Figure S5).

Following the same procedure at Section 3.2, the mutant strains were induced and then harvested. The cells were re-suspended using Tris-HCl buffer (50 mM, pH 8.0) and then the resulting re-suspension was disrupted through ultrasonication. The cell lysates were centrifuged at $8000\times g$ for 10 min, and the supernatant was defined as crude enzyme. The catalytic performance of crude enzyme was investigated in 5 mL reaction mixture containing 100 mM methyl glycolate, 0.01 mM FMN and 10 mg crude enzyme. The reaction was conducted at 25 °C and 600 rpm. After 8 h reaction, the reaction mixture was centrifuged, and the supernatant was subjected to HPLC analyses.

3.5. HPLC Analyses of Methyl Glycolate and Methyl Glyoxylate

The method of HPLC (Waters 1525) equipped with an UV detector (Waters 2489) was established for the determination of methyl glycolate and methyl glyoxylate. The wavelength of the UV detector was 212 nm and the column type was C-18 (Welch, 30 m \times 250 μ m \times 0.25 μ m). The injection volume was 10 μ L and the temperature was set as 40 °C. The mobile phase at a flow rate of 0.5 mL/min was 0.1% (v/v) phosphoric acid solution (pH 2.7). The retention times for methyl glycolate and methyl glyoxylate were 9.655 min and 4.695 min, respectively (Figure S6).

3.6. Site-Saturation Mutagenesis for the Sites M267 and S362 of SoGOX

After the sites M267 and S362 had been proved to be key residues for SoGOX activity, the sites M267 and S362 were simultaneously subjected to site-saturation mutagenesis. Using the plasmid pET28a-SoGOX as template, the fragment between M267 and S362 was PCR-amplified using the pair of primers M267X-F and S362X-R, and the rest part of the plasmid pET28a-SoGOX was amplified through reverse PCR using the pair of primers M267X-R and S362X-F (Table S4). The PCR program included a 5 min period at 95 °C, 30 cycles at 95 °C (15 s), 60 °C (30 s) and 72 °C (60 s for normal PCR or 180 s for reverse PCR), and a final 10 min extension at 72 °C. The PCR products were digested by *Dpn* I to remove the template and then purified. Through Exnase II-derived homologous recombination in the ClonExpress MultiS One Step Cloning Kit, the fragment between M267 and S362 and the rest part of the plasmid were ligated to form the recombinant plasmid carrying the mutation at sites M267 and S362.

3.7. Key Factors on Oxidation of Methyl Glycolate Using Crude Fusion Enzyme VsHGB-GSG-SoGOX^{mut}-GGGGS-HpCAT

Using the plasmid pET28a-VsHGB-GSG-SoGOX-GGGGS-HpCAT as a template, the fragment between M267 and S362 was PCR-amplified using the pair of primers M267T-F and S362G-R, and the rest part of the plasmid pET28a-VsHGB-GSG-SoGOX-GGGGS-HpCAT was amplified through reverse PCR using the pair of primers S362G-F and M267T-R (Table S5). Following the same procedure in Section 3.6, the products from normal and reverse PCRs were ligated to form the recombinant plasmid pET28a-VsHGB-GSG-SoGOX^{mut}-GGGGS-HpCAT. The plasmid pET28a-VsHGB-GSG-SoGOX^{mut}-GGGGS-HpCAT was transformed into the host strain *E. coli* BL21(DE3), giving the recombinant strain *E. coli* BL21(DE3)/pET28a-VsHGB-GSG-SoGOX^{mut}-GGGGS-HpCAT. The induction of the strain was initiated by the addition of 0.6 mM IPTG and then it was cultured at 20 °C for 12 h. The cells were washed twice using Tris-HCl buffer (50 mM, pH 8.0), and harvested by $8000\times g$ centrifugation at 4 °C for 10 min. The cells were re-suspended using Tris-HCl buffer (50 mM, pH 8.0) and then the resulting

re-suspension was disrupted through ultrasonication. The cell lysates were centrifuged at 8000× g for 10 min, and the supernatant was defined as crude enzyme.

The standard reaction mixture (5 mL) contained 100 mM methyl glycolate, 0.01 mM FMN and 10 mg crude enzyme. The reaction at an oxygen aeration rate of 1 L/h was conducted at 25 °C and 600 rpm for 6 h. The factors were individually varied to test the effect on the oxidation of methyl glycolate. The optimal temperature of alcohol oxidation was explored by varying the temperatures from 5 to 40 °C. The optimal pH was investigated at pH values ranging from pH 6.0 to 10. The buffers used were piperazine-1,4-bisethanesulfonic acid (PIPES, pH 6.0, 6.5 and 7.0), Tris-HCl (pH 7.5, 8.0, 8.5 and 9.0) and *N*-cyclohexyl-3-aminopropanesulfonic acid (CAPS, pH 9.5 and 10.0). The aeration rates of oxygen were explored within the range of 0 to 3 L/h. The concentrations of FMN were tested within the range of 0 to 0.2 mM. The concentrations of substrate were stepwise increased from 50 to 400 mM. After 6 h reaction, the reaction mixture was centrifuged and the supernatant was subjected to HPLC analysis.

4. Conclusions

Rather than the oxidation of glycolic acid, this study developed enzymatic oxidation of methyl glycolate to methyl glyoxylate through cascade catalysis of glycolate oxidase, catalase and hemoglobin. The reaction yield in enzymatic oxidation of methyl glycolate was enhanced through the fusion over-expression of *SoGOX*, *HpCAT* and *VsHGB*, directed evolution of *SoGOX* and the orchestration of reaction conditions. It should be noted that the use of crude enzyme virtually eliminated side reactions and made it possible to prepare large quantities of the biocatalyst in a simple and economical way. When all the improvements were integrated, the 6 h oxidation of 200 mM methyl glycolate catalyzed by crude fusion enzyme *VsHGB-GSG-SoGOX^{mut}-GGGGS-HpCAT* resulted in a yield of 95.3%, opening the possibility of employing enzymatic oxidation of methyl glycolate to methyl glyoxylate in a preparative scale.

Supplementary Materials: The following are available online at <http://www.mdpi.com/2073-4344/10/8/943/s1>, Figure S1: The GC and GC-MS analyses of methyl glycolate and methyl glyoxylate, Figure S2: The structure of *SoGOX* and its mutation site, Figure S3: The procedure for the construction of the recombinant plasmid pET28a-*VsHGB-GSG-SoGOX-GSG-HpCAT*, Figure S4: The colorimetric assay for the determination of H₂O₂, Figure S5: Primary screening of the evolved mutants based on the detection of H₂O₂, Figure S6: HPLC chromatogram of methyl glycolate (a) and methyl glyoxylate (b), Table S1: The primers for the construction of the fusion genes encoding *VsHGB-linker-SoGOX-linker-HpCAT*, Table S2: The primers for the construction of the fusion genes encoding *HpCAT-linker-SoGOX-linker-VsHGB*, Table S3: The primers for directed evolution of *SoGOX*, Table S4: The primers for site-saturation mutagenesis at sites M267 and S362 of *SoGOX*, Table S5: The primers for the construction of the recombinant plasmid pET28a-*VsHGB-GSG-SoGOX^{mut}-GGGGS-HpCAT*.

Author Contributions: Conceptualization, X.Y.; Methodology, X.Y.; C.W.; Validation, X.Y., C.W. and S.S.; Formal Analysis, C.W., S.S. and Q.W.; Investigation, C.W., S.S., Q.W., X.Z., L.C., C.L. and M.Z.; Resources, X.Y.; Data Curation, X.Y.; Writing-Original Draft Preparation, X.Y.; C.W.; Writing-Review and Editing, X.Y.; Visualization, X.Y.; C.W.; Supervision, Y.B.; Z.W.; Project Administration, X.Y.; Funding Acquisition, X.Y. All authors have read and agreed to the published version of the manuscript.

Funding: This research was funded by the Natural Science Foundation of Zhejiang Province, China (No. LY17B020012).

Conflicts of Interest: The authors declare no conflict of interest.

References

1. Hook, J.M. A simple and efficient synthesis of ethyl and methyl glyoxylate. *Synth. Commun.* **1984**, *14*, 83–87. [[CrossRef](#)]
2. Bailey, P.D.; Brown, G.R.; Korber, F.; Reed, A.; Wilson, R.D. Asymmetric synthesis of pipercolic acid derivatives using the aza-Diels-Alder reaction. *Tetrahedron Asymmetry* **1991**, *2*, 1263–1282. [[CrossRef](#)]
3. Ying, X.; Yu, S.; Huang, M.; Wei, R.; Meng, S.; Cheng, F.; Yu, M.; Ying, M.; Zhao, M.; Wang, Z. Engineering the enantioselectivity of yeast old yellow enzyme OYE2y in asymmetric reduction of (*E/Z*)-citral to (*R*)-citronellal. *Molecules* **2019**, *24*, 1057. [[CrossRef](#)] [[PubMed](#)]

4. Zhou, J.; Chen, Z.; Wang, Y. Bioaldehydes and beyond: Expanding the realm of bioderived chemicals using biogenic aldehydes as platforms. *Curr. Opin. Chem. Biol.* **2020**, *59*, 37–46. [[CrossRef](#)] [[PubMed](#)]
5. Heidlindemann, M.; Hammel, M.; Scheffliffllfler, U.; Mahrwald, R.; Hummel, W.; Berkessel, A.; Gröger, H. Chemoenzymatic synthesis of vitamin B5-intermediate (R)-pantolactone via combined asymmetric organo- and biocatalysis. *J. Org. Chem.* **2015**, *80*, 3387–3396. [[CrossRef](#)]
6. Monti, D.; Ottolina, G.; Carrea, G.; Riva, S. Redox reactions catalyzed by isolated enzymes. *Chem. Rev.* **2011**, *111*, 4111–4140. [[CrossRef](#)]
7. Kroutil, W.; Mang, H.; Edegger, K.; Faber, K. Biocatalytic oxidation of primary and secondary alcohols. *Adv. Synth. Catal.* **2004**, *346*, 125–142. [[CrossRef](#)]
8. Liu, J.; Wu, S.; Li, Z. Recent advances in enzymatic oxidation of alcohols. *Curr. Opin. Chem. Biol.* **2018**, *43*, 77–86. [[CrossRef](#)]
9. Jin, J.; Tan, T.; Wang, H.; Su, G. The Expression of spinach glycolate oxidase (GO) in *E. coli* and the application of GO in the production of glyoxylic acid. *Mol. Biotechnol.* **2003**, *25*, 207–214. [[CrossRef](#)]
10. Isobe, K.; Watabe, S.; Yamada, M. Characterization and application of a glycolate dehydrogenase from *Trichoderma harzianum* AIU 353. *J. Mol. Catal. B Enzym.* **2012**, *83*, 94–99. [[CrossRef](#)]
11. Nölke, G.; Houdelet, M.; Kreuzaler, F.; Peterhänsel, C.; Schillberg, S. The expression of a recombinant glycolate dehydrogenase polyprotein in potato (*Solanum tuberosum*) plastids strongly enhances photosynthesis and tuber yield. *Plant Biotechnol. J.* **2014**, *12*, 734–742. [[CrossRef](#)] [[PubMed](#)]
12. Yamada, M.; Higashiyama, T.; Kishino, S.; Kataoka, M.; Ogawa, J.; Shimizu, S.; Isobe, K. Novel alcohol oxidase with glycolate oxidase activity from *Ochrobactrum* sp. AIU 033. *J. Mol. Catal. B Enzym.* **2014**, *105*, 41–48. [[CrossRef](#)]
13. Dellerio, Y.; Mauve, C.; Boex-Fontvieille, E.; Flesch, V.; Jossier, M.; Tcherkez, G.; Hodges, M. Experimental evidence for a hydride transfer mechanism in plant glycolate oxidase catalysis. *J. Biol. Chem.* **2015**, *290*, 1689–1698. [[CrossRef](#)] [[PubMed](#)]
14. de Almeida, T.P.; van Schie, M.M.C.H.; Ma, A.; Tieves, F.; Younes, S.H.H.; Fernández-Fueyo, E.; Arends, I.W.C.E.; Riul, A., Jr.; Hollmanna, F. Efficient aerobic oxidation of trans-2-hexen-1-ol using the aryl alcohol oxidase from *Pleurotus eryngii*. *Adv. Synth. Catal.* **2019**, *361*, 2668–2672. [[CrossRef](#)]
15. Gavagan, J.E.; Fager, S.K.; Seip, J.E.; Payne, M.S.; Anton, D.L.; DiCosimo, R. Glyoxylic acid production using microbial transformant catalysts. *J. Org. Chem.* **1995**, *60*, 3957–3963. [[CrossRef](#)]
16. Ricca, E.; Brucher, B.; Schrittwieser, J.H. Multi-enzymatic cascade reactions: Overview and perspectives. *Adv. Synth. Catal.* **2011**, *353*, 2239–2262. [[CrossRef](#)]
17. Li, G.; Lian, J.; Xue, H.; Jiang, Y.; Wu, M.; Lin, J.; Yang, L. Enzymatic preparation of pyruvate by a whole-cell biocatalyst coexpressing L-lactate oxidase and catalase. *Process Biochem.* **2020**, *96*, 113–121. [[CrossRef](#)]
18. Luo, H.; Ji, Q.; Chang, Y.; Du, C. Expression and characterization of fusion protein of *Vitreoscilla hemoglobin* with spinach glycolate oxidase. In Proceedings of the 2011 International Conference on Remote Sensing, Environment and Transportation Engineering, Nanjing, China, 24 June 2011; pp. 7580–7583.
19. Aalbers, F.S.; Fraaije, M.W. Enzyme fusions in biocatalysis: Coupling reactions by pairing enzymes. *ChemBioChem* **2019**, *20*, 20–28. [[CrossRef](#)]
20. Kataoka, M.; Miyakawa, T.; Shimizu, S.; Tanokura, M. Enzymes useful for chiral compound synthesis: Structural biology, directed evolution, and protein engineering for industrial use. *Appl. Microbiol. Biotechnol.* **2016**, *100*, 5747–5757. [[CrossRef](#)]
21. Markel, U.; Essani, K.D.; Besirlioglu, V.; Schifffels, J.; Streit, W.R.; Schwaneberg, U. Advances in ultrahigh-throughput screening for directed enzyme evolution. *Chem. Soc. Rev.* **2020**, *49*, 233–262. [[CrossRef](#)]
22. Hazell, S.L.; Evans, D.J., Jr.; Graha, D.Y. *Helicobacter pylori* catalase. *J. Gen. Microbiol.* **1991**, *137*, 57–61. [[CrossRef](#)] [[PubMed](#)]
23. Khosla, C.; Bailey, J.E. Characterization of the oxygen-dependent promoter of the *Vitreoscilla hemoglobin* gene in *Escherichia coli*. *J. Bacteriol.* **1989**, *171*, 5995–6004. [[CrossRef](#)]
24. Volokita, M.; Somervillet, R.C. The primary structure of spinach glycolate oxidase from the DNA sequence of a cDNA clone. *J. Biol. Chem.* **1987**, *262*, 15825–15828.
25. Macheroux, P.; Mulrooney, S.B.; Williams, C.H., Jr.; Massey, V. Direct expression of active spinach glycolate oxidase in *Escherichia coli*. *Biochim. Biophys. Acta* **1992**, *1132*, 11–16. [[CrossRef](#)]
26. Macheroux, P.; Massey, V.; Thiele, D.J. Expression of spinach glycolate oxidase in *Saccharomyces cerevisiae*: Purification and characterization. *Biochemistry* **1991**, *30*, 4612–4619. [[CrossRef](#)] [[PubMed](#)]

27. Stenberg, K.; Lindqvist, Y. High-level expression, purification, and crystallization of recombinant spinach glycolate oxidase in *Escherichia coli*. *Protein Expr. Purif.* **1996**, *8*, 295–298. [[CrossRef](#)]
28. Guo, H.; Yang, Y.; Xue, F.; Zhang, H.; Huang, T.; Liu, W.; Liu, H.; Zhang, F.; Yang, M.; Liu, C.; et al. Effect of flexible linker length on the activity of fusion protein 4-coumaroyl-CoA ligase: Stilbene synthase. *Mol. BioSyst.* **2017**, *13*, 598–606. [[CrossRef](#)]
29. Aalbers, F.S.; Fraaije, M.W. Design of artificial alcohol oxidases: Alcohol dehydrogenase-NADPH oxidase fusions for continuous oxidations. *ChemBioChem* **2019**, *20*, 51–56. [[CrossRef](#)]
30. Ge, M.; Chi, X.; Zhang, A.; Luo, G.; Sun, G.; Xie, H.; Hei, Z. Intestinal NF-E2-related factor-2 expression and antioxidant activity changes in rats undergoing orthotopic liver autotransplantation. *Oncol. Lett.* **2013**, *6*, 1307–1312. [[CrossRef](#)]
31. Hiraka, K.; Kojima, K.; Tsugawa, W.; Asano, R.; Ikebukuro, K.; Sode, K. Rational engineering of *Aerococcus viridans* L-lactate oxidase for the mediator modification to achieve quasi-direct electron transfer type lactate sensor. *Biosens. Bioelectron.* **2020**, *151*, 111974. [[CrossRef](#)]
32. Dick, M.; Hartmann, R.; Weiergraber, O.H.; Bisterfeld, C.; Classen, T.; Schwarten, M.; Neudecker, P.; Willbold, D.; Pietruszka, J. Mechanism-based inhibition of an aldolase at high concentrations of its natural substrate acetaldehyde: Structural insights and protective strategies. *Chem. Sci.* **2016**, *7*, 4492–4502. [[CrossRef](#)] [[PubMed](#)]
33. Kadkhodaei, S.; Memari, H.R.; Abbasiliasi, S.; Rezaei, M.A.; Movahedi, A.; Shung, T.J.; Ariff, A.B. Multiple overlap extension PCR (MOE-PCR): An effective technical shortcut to high throughput synthetic biology. *RSC Adv.* **2016**, *6*, 66682. [[CrossRef](#)]



© 2020 by the authors. Licensee MDPI, Basel, Switzerland. This article is an open access article distributed under the terms and conditions of the Creative Commons Attribution (CC BY) license (<http://creativecommons.org/licenses/by/4.0/>).